Absolute Polarization Measurement Using a Vector Light Shift

Kunyan Zhu, Neal Solmeyer, Cheng Tang, and David S. Weiss

Physics Department, The Pennsylvania State University, 104 Davey Laboratory, University Park, Pennsylvania 16802, USA

(Received 6 September 2013; published 12 December 2013)

We have measured the vector light shift due to a cavity built-up optical lattice by using a variation of the Hanle effect with trapped Cs atoms, where the time-evolving population of all magnetic sublevels is measured *in situ*. The measurement is linearly sensitive to the electric field of the nonlinearly polarized light, which allows unprecedented sensitivity to absolute linear polarization quality, to the level of 10^{-10} in fractional intensity. Our approach to measuring and improving linear polarization can be applied to electron electric dipole moment searches, optical lattice clocks, magnetometery, and quantum computing.

DOI: 10.1103/PhysRevLett.111.243006 PACS numbers: 32.60.+i, 37.10.Jk, 42.25.Ja

Vector light shifts (VLSs), which are ac-Stark shifts proportional to an atom's magnetic quantum number, act on atoms like fictitious magnetic fields. They are the basis for the study of ultracold atoms in synthetic gauge fields [1], they can be employed to move atoms in optical lattices [2,3], and they provide a way to cancel the effect of real magnetic fields in some precision measurements [4,5]. Spatial variations of VLSs have been used for NMR [6]. But spatial variations can also create unwanted inhomogeneous frequency shifts, making VLSs a troublesome complication in precision measurements. VLSs are an unwanted background in magnetic field measurements [7,8]. In measurements that require small, well-controlled magnetic fields, such as atomic clocks [9] and electric dipole moment searches [10–12], VLSs can result in poorly controlled frequency shifts. The long coherence times that are desired for quantum information processing can be more difficult to attain because of the VLS [13,14].

Experiments can often be designed to minimize the adverse effect of VLSs due to trapping light [8–10,12], but the VLS would be avoided altogether if pure linear polarization could be used. There is a huge body of physics and engineering work concerned with the measurement of small polarization changes [15–19]. For instance, in recent work aimed at measuring the birefringence of the vacuum in large magnetic fields, relative polarization changes as small as 3×10^{-13} rad have been measured [17]. But sensitivity to small polarization changes does not readily translate into sensitivity to absolute polarization.

High sensitivity to polarization changes generally requires measuring the interference cross term from the sum of a large reference field and the smaller field that is changing. A simple example of such a measurement consists of sending a mostly linearly polarized beam at 45° into a polarizing beam splitter and detecting the difference of the outputs from the two ports. Such a measurement is linearly sensitive to electric field rotation but is insensitive to ellipticity. An absolute linear polarization measurement along the same lines requires the use of light that is mostly polarized along one of the prism axes, which makes the signal only quadratically sensitive to the wrong component of the electric field. The best Glan-laser prisms (GLPs) can distinguish as little as 10^{-6} of the wrong intensity, which corresponds to only 10^{-3} rad deviation of the electric field from linear polarization. The best nanoparticle polarizers can have an order of magnitude better extinction ratios [20] than GLPs, but with a damage threshold of $\sim 10^5$ W/m^2 they can be used only in low power applications. It is hard to do better, because of residual birefringence in optical elements and low-level scattering, which introduces unwanted momentum and hence polarization components into a beam [15,16].

In work presented here, we use the VLS on cold atoms to achieve a sensitivity to absolute linear polarization that, like experiments that measure small polarization changes, is linearly sensitive to the electric field. This in turn allows us to demonstrate the creation of the very high quality linear polarization that we need to make the VLS small. We improve the linear polarization of optical lattice beams by building up the light in a Fabry-Perot cavity. The cavity filters out spatial noise introduced by scatterers, and in-cavity Brewster plates filter out the wrong polarization components. Since our cavity contains slightly birefringent vacuum windows [21] and has only a modest build-up factor, it is possible that other experiments have produced better linear polarizations. But by measuring the VLS via a variation of the Hanle effect [22,23] on cold trapped atoms, we can measure the absolute linear polarization with unprecedented sensitivity and obtain linear polarizations better than the best GLPs.

The VLS for a ground state atom in a far off-resonant trap is [24,25]

$$\nu_V = \alpha_V(\lambda) U m_F (i\boldsymbol{\epsilon}^* \times \boldsymbol{\epsilon}) \cdot \mathbf{e}, \tag{1}$$

where U is the trap depth, $\boldsymbol{\epsilon}$ is the polarization vector, and $\mathbf{e}$ is the quantization axis. $\alpha_V(\lambda)$ is 464 Hz/μK for the Cs $F = 3$ hyperfine ground state and $\lambda = 1064$ nm trapping light [10]. Maximum sensitivity to polarization quality requires that $\mathbf{e}$ be parallel to the wave vector $\mathbf{k}$, which is also the direction of the fictitious magnetic field. Linearly

polarized light propagating along $\mathbf{z}$ with a slightly circular component can be described by

$$\boldsymbol{\epsilon} = \sin\left(\frac{\pi}{4}+\theta\right)\boldsymbol{\epsilon}_L + \exp(i\phi)\cos\left(\frac{\pi}{4}+\theta\right)\boldsymbol{\epsilon}_R, \quad (2)$$

where the small angle θ characterizes the linear polarization quality, the circular polarization vectors $\boldsymbol{\epsilon}_{L,R}$ are given by $\boldsymbol{\epsilon}_L = -(\boldsymbol{\epsilon}_x + i\boldsymbol{\epsilon}_y)/\sqrt{2}$ and $\boldsymbol{\epsilon}_R = (\boldsymbol{\epsilon}_x - i\boldsymbol{\epsilon}_y)/\sqrt{2}$, respectively, and ϕ is the misalignment of the linear polarization with respect to $\boldsymbol{\epsilon}_x$. The angular dependence of the VLS in Eq. (1) is thus $\delta_{VLS} = (i\boldsymbol{\epsilon}^* \times \boldsymbol{\epsilon}) \cdot \mathbf{e} \simeq 2\theta$, linearly sensitive to θ. Imperfect linear polarization corresponds to an excess in one of the circular polarization components, which interferes with the rest of the light of the same circular polarization. Meanwhile, the two equal circular polarization components give exactly canceling shifts on the atom. So unlike the linear-in-θ (i.e., linear-in-E) signal in conventional polarimeters, the linear-in-θ VLS signal sits on zero background.

Our apparatus was partly described in Ref. [11] and is shown schematically in Fig. 1. We first launch and load atoms [11] into two parallel one-dimensional optical lattices in a magnetically shielded measurement region. The parallel lattices geometry is motivated by our electron electric dipole moment (eEDM) measurement; here it

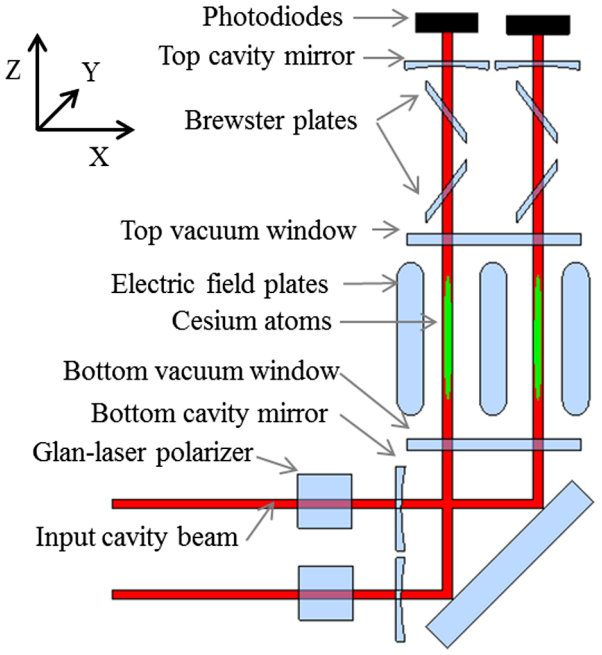

FIG. 1 (color online). Schematic of the experimental setup (not to scale). Laser-cooled atoms are trapped in two parallel 1D optical lattices made in 2-m-long build-up cavities, separated by 1 cm. The 1064 nm input cavity beam polarizations are cleaned up by GLPs. Each cavity contains two low-birefringence vacuum windows and a pair of Brewster plates for cavity locking and polarization purification. The 90° cavity-folding mirror is necessitated by geometric constraints.

provides two independent measurements of the VLS. The 1-cm-separated lattices have a maximum depth of $U_0 \sim k_B \times 160\ \mu$K (where k_B is the Boltzmann constant) and $w = 580\ \mu$m transverse widths. They are made from 1064 nm light in 2-m-long build-up cavities, with a finesse of 300 and a power build-up factor of 25. Each lattice is loaded with approximately 5×10^6 atoms distributed over 5 cm vertically. The eEDM field plates here serve to optically isolate the two lattices from each other. We laser cool the lattice-trapped atoms to a temperature of $T \sim 11\ \mu$K [26]. With resonant, circularly polarized beams that propagate close to the $\mathbf{z}$ axis, along the initial 20 mG B-field direction, we optically pump the atoms into the $|F = 4, m_F = +4\rangle$ magnetic sublevel with 99.97% efficiency. We use an adiabatic fast passage (AFP) microwave pulse [27] to transfer the atoms with 99.5% fidelity into the $|3, +3\rangle$ state. We complete the state preparation by adiabatically switching to a bias field of $B_y = 20$ mG, so the atoms are maximally polarized along $\mathbf{y}$.

We start the Hanle measurement by shutting off the bias field in 5 μs, much faster than the fastest Larmor precession out of $\mathbf{y}$, leaving the atoms in a much smaller effective B_z field. We let the atoms evolve for a time t, during which time they Larmor precess at the composite frequency $\omega = \omega_B + \omega_U$, where ω_B is due to either a real magnetic field and/or a lattice-independent, fictitious magnetic field and ω_U is due to the VLS from the optical lattice light. We then quickly turn on a 20 mG B_x (or B_y). With the atoms thus projected into this new basis, we adiabatically reorient the field along the optical pumping beam direction. We next sequentially measure the populations N_{m_F} of each of the m_F levels. This is done by using a microwave AFP pulse to drive atoms from a single $|3, m_F\rangle$ state to the $|4, m_F\rangle$, followed by a 0.3-ms-long optical detection pulse, using a σ^+-polarized beam in the optical pumping direction, resonant with $F = 4 \rightarrow F' = 5$ and well above saturation intensity. We collect the fluorescence on 1D photodiode arrays [28]. A 2-ms-long clearing pulse then pushes the $F = 4$ atoms out of the detection region. We repeat this procedure for all seven levels, giving us a complete picture of the evolution of atoms in the $F = 3$ state during Larmor precession [29]. Figure 2 shows a typical example of the measured population evolution of all seven Zeeman sublevels, along with the corresponding theoretical curves [30].

We define the normalized total atomic spin as

$$S \equiv \frac{1}{(m_F)_{\text{prep}}} \frac{\sum m_F N_{m_F}}{\sum N_{m_F}}, \quad (3)$$

where the initially prepared state is $(m_F)_{\text{prep}} = +3$ and the summation goes from $m_F = -3$ to $m_F = +3$. Using the Wigner D-rotation matrix [31], one can show that, ideally, $S = \cos(\omega t)$ if in the final step we measure along $\mathbf{y}$ and $S = \sin(\omega t)$ if we measure along $\mathbf{x}$ [30]. Figure 3 shows spin precessions $S(t)$ when we purposely make ω_U greatly exceed ω_B, illustrated by the fact that halving the lattice

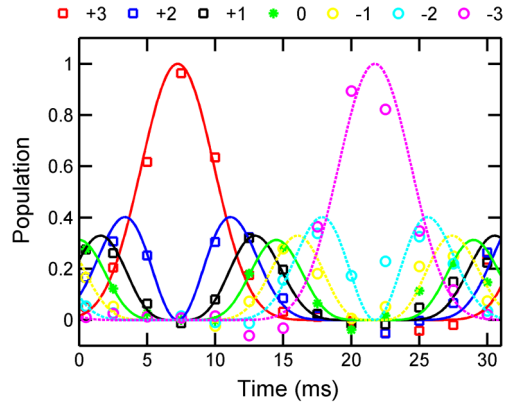

FIG. 2 (color online). Population evolution for all seven $F = 3$ Zeeman sublevels during a Larmor precession cycle in an effective magnetic field of 100 μG. Spins are prepared in **y** and measured in **x**. The lines are theoretical predictions without dephasing (which is quantified later in the Letter). Each set of seven points is from a single atom ensemble. The standard deviation of ± 0.05 in fractional population is dominated by fluctuations in the background from scattered trapping light. Imperfect background substraction due to these fluctuations can lead to an inference of negative populations. These fluctuations can be avoided in future measurements with an additional 1064 nm filter.

power halves the oscillation frequency. The oscillations quickly damp out, because trapped atoms with different energies experience different average VLSs.

We have constructed two models for $S(t)$ to account for this inhomogeneity. The first applies to Fig. 3, for which ω exceeds the transverse oscillation frequency, $\omega_\rho \simeq 2\pi \times 31$ Hz (when $U_0 = k_B \times 100$ μK), and is much less than

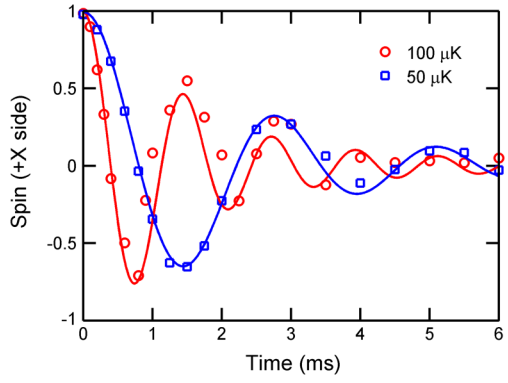

FIG. 3 (color online). Measured spin precession for two different trap depths: $U_0 = k_B \times 100$ μK (red circles) and $U_0 = k_B \times 50$ μK (blue squares). For illustrative purposes, ω_U is made much larger than ω_B for this measurement. The atoms are prepared in state $|3, +3\rangle$ along **y**, are allowed to spin precess along **z**, and are then measured along **y**. Lowering the trap depth by half decreases the precession frequency by a factor of 2. Points on the two curves are taken alternately to minimize any effect of small ω_B drifts. Numerical fitting (solid lines) to Eq. (5) implies a vector light shift of 792 ± 30 Hz for a 100 μK trap depth.

the axial oscillation frequency, $\omega_z \simeq 2\pi \times 105$ kHz. Atoms are spread out axially according to harmonic oscillator wave functions, while their transverse positions are essentially fixed on this time scale. The spatial dependence of the precession is given by $\omega(\rho, n_z) \simeq \omega_{U_0} g(n_z)(1 - \rho^2/w^2)$, where ω_{U_0} is the peak ω_U and $g(n_z) = [1 - \frac{1}{2}(n_z + \frac{1}{2})(\hbar\omega_z/U_0)]$, where the virial theorem has been used to account for the average intensity in each axial mode, n_z. For the approximately thermal distribution that results from laser cooling [26], the transverse spatial distribution is given by $f(\rho) \simeq \exp(-\rho^2/2\sigma_\rho^2)/\sqrt{2\pi\sigma_\rho^2}$, where $\sigma_\rho = \omega_\rho^{-1}\sqrt{k_B T/m}$ is the transverse width and the axial occupation probabilities are given by $p(n_z) \propto e^{-n_z\hbar\omega_z/k_B T}$. The observed spin precession is the weighted spatial average,

$$S(t) = \sum_{n_z} p(n_z) \int \cos\{[\omega_B + \omega_U(\rho, n_z)]t\} f(\rho) d\rho. \quad (4)$$

The integral can be simplified to yield

$$S(t) = \sum_{n_z} p(n_z) \frac{\cos[(a + \omega_B)t - \arctan(bt)]}{\sqrt{1 + (bt)^2}}, \quad (5)$$

where $a = \omega_{U_0} g(n_z)$ and $b = (k_B T/U_0)a$. Three free parameters are used to simultaneously fit the two precession curves in Fig. 3 to Eq. (5): the normalized peak VLS ω_{U_0}/U_0; the normalized temperature $T/\sqrt{U_0}$, which assumes that U_0 is adiabatically changed after cooling; and ω_B. From the fit value of ω_{U_0} we determine that the peak vector light shift is 792 ± 30 Hz, which implies a polarization defect of $\theta = 7.3 \times 10^{-3}$ rad. The fit temperature value gives $T = 21.6 \pm 1.3$ μK (for $U_0 = k_B \times 100$ μK). *In situ* imaging of cooling light implies a transverse temperature of $T = 11.0 \pm 0.8$ μK. The discrepancy suggests that the polarization quality varies across the lattice beams. That the model does not explicitly account for this does not significantly affect the value of ω, which changes by only 4.9%, comparable to the fit uncertainty, when we fit by using the measured temperature.

Spin precession data for our best polarization [32] are shown in Fig. 4 for both optical lattices, with detection in the **x** direction. Since ω is comparable to ω_ρ and smaller than ω_z, we calculate $S(t)$ in a somewhat different way, assuming that the atoms sample their whole transverse orbits during a spin precession. The result is

$$S(t) = \sum_{n_\rho, n_z} p(n_\rho) p(n_z) \sin\{[\omega_B + \omega_U(n_\rho, n_z)]t\}, \quad (6)$$

where $n_\rho = n_x + n_y$, $p(n_\rho) \propto (n_\rho + 1)e^{-n_\rho\hbar\omega_\rho/k_B T}$ is the Boltzmann distribution of transverse modes, and $\omega_U(n_\rho, n_z) = \omega_{U_0}[1 - \frac{1}{2}(n_\rho + 1)(\hbar\omega_\rho/U_0) - \frac{1}{2}(n_z + \frac{1}{2})(\hbar\omega_z/U_0)]$ is the average ω for the mode number (n_ρ, n_z). We find that this quantum mechanical approach makes it easy to average over all semiclassical atom trajectories, at

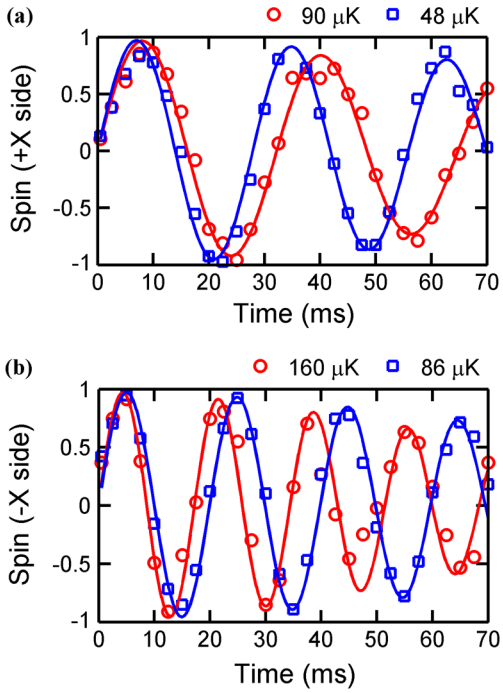

FIG. 4 (color online). Measured spin precession at two different lattice depths in the (a) $+X$ and (b) $-X$ lattices. All cavity elements are aligned for optimum linear polarization. The atoms are prepared in $|3,+3\rangle$ along $\mathbf{y}$, spin precess along $\mathbf{z}$ due to a combination of ω_B and ω_U, and are finally measured along $\mathbf{x}$. Numerical fitting (solid lines) to Eq. (6) implies vector light shifts of -13.9 ± 0.5 Hz $(+X)$ and 12.3 ± 0.4 Hz $(-X)$ for a 100 μK trap depth. The signs are different because the residual circular polarizations of the two lattices have opposite handedness.

the small cost of extra computational time due to the ~60000 occupied modes. As before, we fit the data in Fig. 4 to Eq. (6) for both lattice depths of each lattice simultaneously. Since ω_U is much smaller than ω_B (which fits to $2\pi \times 39.4 \pm 0.4$ and $2\pi \times 43.1 \pm 0.8$ Hz for the $+X$ and $-X$ lattices, respectively), there is little dephasing, and we are not very sensitive to T (a factor of 2 change in T leads to only ~3% change in ω_U). The fit values correspond to polarization imperfections of $\theta_{+X} = -1.5 \times 10^{-4}$ rad and $\theta_{-X} = 1.3 \times 10^{-4}$ rad, or fractional intensity impurities of 2.2×10^{-8} $(+X)$ and 1.8×10^{-8} $(-X)$, about 2 orders of magnitude better than can be measured with a GLP. There is a possible complicated experimental scenario [33] in which the average polarization quality is 3 times worse, but nonlinear effects in our fused silica optics counterbalance polarization imperfections to reduce the inhomogeneous broadening to the size we see in Fig. 4, which also gives rise to ω_B. We estimate that these effects are more than 2 orders of magnitude too small to account for our data, but, since we do not definitively know the source of ω_B, we have not yet empirically ruled out this scenario.

The existing apparatus has a VLS sensitivity at least as small as 1 Hz for a 100 μK trap depth or, equivalently, $\theta \leq 1.1 \times 10^{-5}$ rad. This absolute sensitivity is comparable to the relative sensitivity of commercial interferometric polarimeters [19]. Although we do not know what now limits our polarization quality, the analysis related to Fig. 3 suggests that there are spatial gradients in the polarization, perhaps from spatially dependent birefringence of the intracavity vacuum windows. Further improvement might be had from eliminating the windows or by increasing the cavity Q factor.

In conclusion, we have demonstrated a sensitive technique for measuring VLSs based on atomic spin precession. It allows unprecedented sensitivity to absolute linear polarization quality, to levels as small as 10^{-10} in fractional intensity. We have prepared and measured high power, 1D optical lattices with an absolute linear polarization quality that is at least an order of magnitude better than even the best GLPs. These low VLSs are important for our ongoing eEDM experiment and may impact other optical lattice-based measurements, like optical lattice clocks, magnetometery, quantum computing, and tests of fundamental symmetries.

This work is supported by the National Science Foundation (NSF PHY-11-02737 and PHY-13-07096) and has been supported by the Packard Foundation.

[1] Y.-J. Lin, R. L. Compton, K. Jiménez-García, J. V. Porto, and I. B. Spielman, Nature (London) **462**, 628 (2009).
[2] G. K. Brennen, C. M. Caves, P. S. Jessen, and I. H. Deutsch, Phys. Rev. Lett. **82**, 1060 (1999).
[3] O. Mandel, M. Greiner, A. Widera, T. Rom, T. W. Hänsch, and I. Bloch, Phys. Rev. Lett. **91**, 010407 (2003).
[4] R. Chicireanu, K. D. Nelson, S. Olmschenk, N. Lundblad, A. Derevianko, and J. V. Porto, Phys. Rev. Lett. **106**, 063002 (2011).
[5] Y. O. Dudin, R. Zhao, T. A. B. Kennedy, and A. Kuzmich, Phys. Rev. A **81**, 041805(R) (2010).
[6] I. M. Savukov, S.-K. Lee, and M. V. Romalis, Nature (London) **442**, 1021 (2006).
[7] M. Vengalattore, J. M. Higbie, S. R. Leslie, J. Guzman, L. E. Sadler, and D. M. Stamper-Kurn, Phys. Rev. Lett. **98**, 200801 (2007).
[8] V. I. Yudin, A. V. Taichenachev, Y. O. Dudin, V. L. Velichansky, A. S. Zibrov, and S. A. Zibrov, Phys. Rev. A **82**, 033807 (2010).
[9] J. A. Sherman, N. D. Lemke, N. Hinkley, M. Pizzocaro, R. W. Fox, A. D. Ludlow, and C. W. Oates, Phys. Rev. Lett. **108**, 153002 (2012).
[10] M. V. Romalis and E. N. Fortson, Phys. Rev. A **59**, 4547 (1999).
[11] F. Fang and D. S. Weiss, Opt. Lett. **34**, 169 (2009).
[12] N. Solmeyer, Ph.D. dissertation, Penn State University, 2013.
[13] R. Zhao, Y. O. Dudin, S. D. Jenkins, C. J. Campbell, D. N. Matsukevich, T. A. B. Kennedy, and A. Kuzmich, Nat. Phys. **5**, 100 (2009).
[14] X. Li, T. A. Corcovilos, Y. Wang, and D. S. Weiss, Phys. Rev. Lett. **108**, 103001 (2012).

[15] J. Morville and D. Romanini, Appl. Phys. B **74**, 495 (2002).
[16] G. N. Birich, Yu. V. Bogdanov, S. I. Kanorskii, I. I. Sobelman, V. N. Sorokin, I. I. Struk, and E. A. Yukov, J. Russ. Laser Res. **15**, 455 (1994).
[17] M. Durand, J. Morville, and D. Romanini, Phys. Rev. A **82**, 031803(R) (2010).
[18] G. Zavattini, U. Gastaldi, R. Pengo, G. Ruoso, F. Della valle, and E. Milotti, Int. J. Mod. Phys. A **27**, 1260017 (2012).
[19] B. Wang and T. C. Oakberg, Rev. Sci. Instrum. **70**, 3847 (1999).
[20] For example, see specifications of colorPol® polarizers at http://www.codixx.de/.
[21] N. Solmeyer, K. Zhu, and D. S. Weiss, Rev. Sci. Instrum. **82**, 066105 (2011).
[22] W. Hanle, Z. Phys. **30**, 93 (1924).
[23] D. Budker, W. Gawlik, D. Kimball, S. Rochester, V. Yashchuk, and A. Weis, Rev. Mod. Phys. **74**, 1153 (2002).
[24] B. S. Mathur, H. Tang, and W. Happer, Phys. Rev. **171**, 11 (1968).
[25] I. H. Deutsch and P. S. Jessen, Phys. Rev. A **57**, 1972 (1998).
[26] S. L. Winoto, M. T. DePue, N. E. Bramall, and D. S. Weiss, Phys. Rev. A **59**, R19 (1999).
[27] See Supplemental Material at http://link.aps.org/supplemental/10.1103/PhysRevLett.111.243006 for the AFP pulse parameters.
[28] K. Zhu, N. Solmeyer, and D. S. Weiss, Rev. Sci. Instrum. **83**, 113105 (2012).
[29] G. Klose, G. Smith, and P. S. Jessen, Phys. Rev. Lett. **86**, 4721 (2001).
[30] See Supplemental Material at http://link.aps.org/supplemental/10.1103/PhysRevLett.111.243006 for the theoretical derivations.
[31] M. A. Morrison and G. A. Parker, Aust. J. Phys. **40**, 465 (1987).
[32] See Supplemental Material at http://link.aps.org/supplemental/10.1103/PhysRevLett.111.243006 for methods to optimize the linear polarization.
[33] See Supplemental Material at http://link.aps.org/supplemental/10.1103/PhysRevLett.111.243006 for details of the scenario.